

Article

Authenticating Basil (*Ocimum* spp.): An Integrated Quality Control Strategy

Nazia Nazar¹, Velusamy Sundaresan^{1,2,3}, Ram S. Verma^{3,4}, Adrian Slater¹, Randolph R. J. Arroo⁵ and Tiziana Sgamma^{1,*}

¹ Biomolecular Technology Group, Leicester School of Allied Health Science, Faculty of Health and Life Sciences, De Montfort University, Leicester LE1 9BH, UK

² Plant Biology and Systematics, CSIR—Central Institute of Medicinal and Aromatic Plants, Research Centre, Bengaluru 560065, India

³ Academy of Scientific and Innovative Research (AcSIR), Ghaziabad 201002, India

⁴ Phytochemistry Division, CSIR—Central Institute of Medicinal and Aromatic Plants, Lucknow 226015, India

⁵ Leicester School of Pharmacy, Faculty of Health and Life Sciences, De Montfort University, Leicester LE1 9BH, UK

* Correspondence: Tiziana.sgamma@dmu.ac.uk

How To Cite: Nazar, N.; Sundaresan, V.; Verma, R.S.; et al. Authenticating Basil (*Ocimum* spp.): An Integrated Quality Control Strategy. *Natural Products Analysis* **2025**, *1*(1), 100006. <https://doi.org/10.53941/npa.2025.100006>

Received: 2 September 2025

Revised: 25 September 2025

Accepted: 25 September 2025

Published: 21 October 2025

Abstract: Standardisation is essential to ensure the quality, efficacy, and safety of basil oil products. Although *Ocimum basilicum* L. is the most widely traded species, other *Ocimum* species are often sold under the same name, increasing the risk of misidentification and adulteration. Intraspecific variation in morphology and chemical composition further complicates standardisation, highlighting the need for a comprehensive authentication strategy. This study evaluates genetic, chemical, and morphological methods for the authentication of commercial basil accessions to support accurate species identification and product standardisation. Samples were analysed using DNA barcoding (*matK*, *trnH-psbA*, *rbcL*, *rpl16*), GC-MS-based chemical profiling, and trichome characterisation via scanning electron microscopy. Phylogenetic analysis placed all commercial samples within a broad clade encompassing *O. basilicum*, its hybrids, and related species. Species-specific single nucleotide variations in *matK* and *trnH-psbA* supported the identification of distinct accessions. Notably, liquorice basil showed genetic similarities to non-*basilicum* species, suggesting the need to revisit its classification. Chemical profiling revealed substantial variation in essential oil composition, with some samples dominated by linalool and eugenol, and others by methyl chavicol, raising potential safety concerns. Morphological analysis further highlighted differences in trichome density, particularly in the blue spice variety. The findings underscore the limitations of using a single method for basil authentication and advocate for an integrated approach. DNA barcoding supports species identification, while chemical profiling is essential for chemotype differentiation. Developing reliable DNA markers and incorporating combined analyses into routine quality control can strengthen industry standards for natural product authentication.

Keywords: DNA barcoding; chemical profiling; morphological analysis; authentication; *Ocimum*

1. Introduction

Herbal medicine represents one of the earliest forms of healthcare, forming the foundation of both traditional and modern medical practices [1–5]. The popularity of medicinal and aromatic plants (MAPs) has increased significantly over the past few decades, with demand continuing to grow [6–8]. Plants synthesise a vast array of



Copyright: © 2025 by the authors. This is an open access article under the terms and conditions of the Creative Commons Attribution (CC BY) license (<https://creativecommons.org/licenses/by/4.0/>).

Publisher's Note: Scilight stays neutral with regard to jurisdictional claims in published maps and institutional affiliations.

secondary metabolites, which serve as the basis for commercial products in the pharmaceutical, food, perfume, and cosmetic industries [9–11]. MAPs are integral to both traditional and modern medicinal practices, with approximately 60,000 species globally harvested for their therapeutic properties [12–14].

Despite the extensive use of MAPs, the sector faces numerous challenges that impact the quality and efficacy of herbal medicines [15–17]. One of the major concerns is the prevalence of substitutes and adulterants in the market, which can compromise the safety and effectiveness of final products. Additionally, accurate species identification is critical, as misidentification can lead to ineffective or harmful outcomes [7,18–21]. Variability in the quality of MAPs due to environmental factors and cultivation practices further complicates their use [22,23]. To address these challenges, various regulatory guidelines have been established. The World Health Organization (WHO) provides standards to ensure that MAPs are cultivated, harvested, and processed in ways that preserve their medicinal and aromatic properties [1]. The International Fragrance Association (IFRA) plays a critical role in regulating the safe use of fragrance ingredients, including essential oils [24], restricting or prohibiting substances that pose potential health risks, such as allergens or toxic compounds. Additionally, the International Organization for Standardization (ISO) sets key benchmarks for essential oils, covering purity, composition, and labelling, as seen in standards like ISO 9235 [25]. The European Pharmacopoeia further provides monographs detailing quality testing, storage, and identification requirements to ensure that medicinal plants and their derivatives meet stringent quality standards [26]. Despite these established guidelines, numerous cases and studies have reported instances of adulteration and the presence of harmful compounds in commercial products [7,16,27–29]. These challenges highlight the need for more robust quality control measures to ensure the safety, efficacy, and authenticity of MAP-derived products.

Ocimum basilicum L.(basil), belonging to the family Lamiaceae, is widely used in the cosmetic and personal care, pharmaceutical, and fragrance industries due to its therapeutic properties [30–36]. Basil is cultivated in Asia and the Mediterranean regions, with major exporters including France, Italy, Morocco, and Egypt [37]. In the United Kingdom, fresh basil, dried basil leaves, and basil essential oil are imported from various countries, including Israel, Italy, Egypt, and India [38]. However, challenges persist regarding the quality assurance of basil products.

There are numerous chemotypes and morphotypes of basil, each with unique genetic, chemical, and morphological characteristics, making its taxonomy challenging to resolve [39–45]. While macro-morphological variability is evident among basil species, identification through micro-morphological characteristics becomes difficult when the plant is in powdered form or as essential oils [39,46–53]. Furthermore, there are no clearly defined chemical markers that can reliably differentiate between various basil types [50–54]. Several genomic and DNA barcoding studies have been conducted to distinguish basil from other species within the same genus, or from different species within the family [52–63]. Confusion also arises from the common names used for basil. For example, the names “lime basil” and “lemon basil” refer not only to accessions within *O. basilicum* but also to *O. americanum* L. and *O. × africanum*, respectively. Similarly, in India, the term “holy basil” is used for *O. tenuiflorum* Burm.f., a distinct species with significant medicinal significance, which can lead to misidentification [63]. Beyond taxonomic challenges, certain compounds present in basil raise safety concerns. Eugenol, a key component, acts as dermal sensitizer even when present below threshold levels, while methyl eugenol and chavicol are classified as carcinogenic by IFRA, further complicating quality assurance [64–67]. This study aims to evaluate genetic, chemical, and morphological approaches for the authentication of *O.basilicum* species, cultivars, and hybrids in commercial basil products. By assessing the effectiveness of each method, the research seeks to support the development of reliable tools for species identification and quality control, with relevance to the herbal, pharmaceutical, and essential oil industries.

2. Materials and Methods

2.1. Sample Collection

Seeds of various commercial basil accessions (referred to as “tested samples” henceforth) were obtained from different sources. The plants were grown in the glasshouse at De Montfort University, Leicester. Specific details regarding the sources and names of the basil tested samples are outlined in Table 1.

Table 1. Description provided on the labels of tested samples used in the study.

Sample Name	Source	Name of Species (Specified on the Label)
Blue Spice	Premier Seeds Direct	<i>O. basilicum</i>
Dark opal basil	Premier Seeds Direct	<i>O. basilicum purpurascens</i>
Dwarf Greek basil	Premier Seeds Direct	<i>O. basilicum</i>
Lemon Basil	De Ree	<i>O. basilicum citriodorum</i>
Lettuce leaf basil	Magic Garden Seeds	<i>O. basilicum</i>
Lime basil	Premier Seeds Direct	<i>O. basilicum</i>
Liquorice basil	Premier Seeds Direct	<i>O. basilicum</i>
Sweet basil ‘Genovese’	Magic Garden Seeds	<i>O. basilicum</i>
Thai large leaf	Premier Seeds Direct	<i>O. basilicum</i>
Siam Queen Basil	Premier Seeds Direct	<i>O. basilicum</i>

2.2. Genetic Analysis

2.2.1. DNA Isolation and Amplification

Total genomic DNA of each accession was extracted from 100 mg of frozen material, previously ground to a fine powder in liquid nitrogen with mortar and pestle, using DNeasy Plant Mini Kit (Qiagen Inc., Germantown, MD, USA) following the manufacturer’s guidelines.

Polymerase chain reaction (PCR) was performed using a master mix consisting of 1X MyTaq Red Mix, 0.2 µM forward and reverse primers (Table 2), 2 µL of template DNA, making up a final reaction volume of 50 µL with distilled water. A positive control (known DNA sample) and a negative control (distilled water) were always used to ensure the PCR had worked successfully and there was no contamination.

The PCR conditions were as follows: initial denaturation for 5 min at 95 °C, followed by 35 cycles of 1 min at 95 °C, with annealing times of 40 s at 44 °C for *matK*, 30 s at 58 °C for *trnH-psbA*, 20 s at 52 °C for *rbcL*, and 60 s at 52 °C for *rpl16*. The extension step was performed for 1 min at 72 °C. A final extension was carried out for 5 min at 72 °C for all markers.

Table 2. Primers used for amplifying different barcode regions.

Name	Sequence	Amplicon Size (~bp)	Reference
<i>matK</i> -F	5'-CGTACAGTACTTTTGTGTTTACGAG-3'	700	[66]
<i>matK</i> -R	5'-ACCCAGTCCATCTGGAAATCTTGTTTC-3'		
<i>trnH-psbA</i> -F	5'-GTTATGCATGAACGTAATGCTC-3'	400	[66]
<i>trnH-psbA</i> -R	5'-CGCGCATGGTGGATTCACAATCC-3'		
<i>rbcL</i> -F	5'-ATGTCACCACAAACAGAGACTAAAGC-3'	570	[66]
<i>rbcL</i> -R	5'-GTAAAATCAAGTCCACCRCG-3'		
<i>Rpl16</i> -F	5'-GCTATGCTTAGTGTGTGACTCGTTG-3'	600	[68]
<i>Rpl16</i> -R	5'-CCCTTCATTCTTCCTCTATGTTG-3'		

2.2.2. Loci and Primers

Four loci from the chloroplast genome—*maturase K* (*matK*), intergenic spacer region of *trnH* and *photosystem II protein D1* (*trnH-psbA*), *ribulose-bisphosphate carboxylase* (*rbcL*), *ribosomal protein L16* (*rpl16*) were tested for their ability to serve as DNA barcodes for differentiating between 10 types of basil. Primers for the amplification of these loci were selected based on previously published studies (as detailed in Table 2).

2.2.3. Sequencing and Analysis

Samples that produced positive PCR results were sent for sequencing. Sequencing services were provided by Macrogen (<http://foreign.macrogen.com/eng/>, accessed on 6 June 2024). The resulting chromatograms were analysed with CLC Bio Main Workbench (Workbench 7) [69] through a comparison of relevant gene sequences from *Ocimum* species, obtained from publicly available databases. The accession numbers of the sequences used in this study are listed in Table 3. Phylogenetic trees were constructed using MEGA 11.0.13 software through the Neighbor-Joining (NJ) method, applying the Kimura 2-Parameter (K2P) model for evolutionary distance estimation [70]. Sequence alignment was performed using MUSCLE with default parameters for multiple sequence alignment within MEGA 11.0.13. For pairwise distance analysis, any positions containing gaps or

missing data were removed using the complete deletion option. The reliability of the clades in the NJ phylogenetic trees was assessed using bootstrap analysis, where 1000 replicates were used to test the support of clade nodes, providing confidence levels for the groupings observed in the tree.

Table 3. NCBI accession numbers of the *O. basilicum* accessions and *Ocimum* species used in this study.

Name	<i>trnH-psbA</i>	<i>matK</i>	<i>rbcL</i>	<i>rp16</i>
<i>O. basilicum</i> Thai Large Leaf	PV389098	PV494194	PV439827	PV389107
<i>O. basilicum</i> Blue Spice	PV389106	PV494195	PV439834	PV389109
<i>O. basilicum</i> Lemon	PV389102	PV494196	PV439829	PV389111
<i>O. basilicum</i> Liquorice	PV389099	PV494197	PV439830	PV389112
<i>O. basilicum</i> Lime	PV389104	PV494198	PV439831	PV389113
<i>O. basilicum</i> Dwarf Greek	PV389100	PV494199	PV439828	PV389110
<i>O. basilicum</i> Dark Opal	PV389103	PV494200	PV439832	PV389114
<i>O. basilicum</i> Lettuce Leaf	PV389101	PV494201	PV439835	PV389115
<i>O. basilicum</i> Sweet Basil	PV389105	PV494202	PV439836	PV389116
<i>O. basilicum</i> Saim Queen	PV389097	PV494203	PV439833	PV389108
<i>O. basilicum</i>	MW582309.1	MF694868.1	MF694752.1	OQ706275.1
<i>O. basilicum</i>	MH069957.1	KC755404.1	MF694751.1	
<i>O. basilicum</i>	KX096042.1	MW150012.1		
<i>O. basilicum</i>	FR726116.1	MN243437.1		
<i>O. basilicum</i>	FR726117.1	MF468160.2		
<i>O. basilicum</i>	KF855613.1	MN243269.1		
<i>O. basilicum</i>	MF457811.1	KC755403.1		
<i>O. basilicum</i>	KU666423.1			
<i>O. basilicum</i>	MH069955.1			
<i>O. basilicum</i> var. <i>purpurascens</i>	JX294427.1			
<i>O. basilicum</i> var. <i>purpurascens</i>	KT338803.1			
<i>O. basilicum</i> × <i>O. kilimandscharicum</i>	MW150023.1	MW150016.1		
<i>O. basilicum</i> × <i>O. kilimandscharicum</i>	MW150022.1	MW150015.1		
<i>O. americanum</i>	MN251662.1	KC755400.1		
<i>O. americanum</i>	MN755613.1	JX465687.1		
<i>O. americanum</i>	MF457814.1			
<i>Ocimum</i> × <i>africanum</i>	JX294428.1	JX465686.1		
<i>Ocimum</i> × <i>africanum</i>	KU707910.1	JX465683.1		
<i>Ocimum</i> × <i>africanum</i>	JX262182.1	KC755405.1		
<i>Ocimum</i> × <i>africanum</i>	KT338802.1			
<i>O. kilimandscharicum</i>	MF457817.1	MW150014.1		
<i>O. kilimandscharicum</i>	MF457815.1	JX465685.1		
<i>O. kilimandscharicum</i>	JX262180.1			
<i>O. gratissimum</i>	KT338808.1	MW150013.1	MF326410.1	NC_057196.1
<i>O. gratissimum</i>	MN816239.1	JX465684.1		
<i>O. gratissimum</i>	JX262181.1			
<i>O. gratissimum</i>	MW150020.1			
<i>O. gratissimum</i>	KR736034.1			
<i>O. tenuiflorum</i>	KX096041.1	OQ798990.1	OL537014.1	MN687904.1
<i>O. tenuiflorum</i>	OM677459.1	JX465680.1	MF326417.1	
<i>O. tenuiflorum</i>	MF457807.1	MW150017.1		
<i>O. tenuiflorum</i>	KU666421.1	JX465682.1		
<i>O. filamentosum</i>	KR735338.1	KR734359.1		
<i>O. filamentosum</i>	KR735702.1	JX465688.1		
<i>O. filamentosum</i>	KR735322.1	KR734494.1		
<i>O. filamentosum</i>	KR735202.1			
<i>O. filamentosum</i>	JX294429.1			
<i>O. campechianum</i>	MF784557.1	MH464371.1		
<i>O. campechianum</i>	HG963580.1	MF379672.1		

2.3. Microscopic Analysis

The Carl Zeiss Evo® HD 15 scanning electron microscope was used to conduct the SEM work on the fresh basil samples under varying magnifications

2.4. Chemical Analysis

2.4.1. Essential Oil Isolation

The essential oil was extracted from freshly harvested foliage of all the tested samples using the hydro-distillation method, employing a Clevenger's apparatus, as previously outlined [46]. The obtained essential oil was collected in de-moistened glass vials and stored in airtight containers for subsequent GC and GC-MS analysis.

2.4.2. GC-MS Analysis

The analysis of the essential oil was performed with GC-MS/MS system (8890 GC with a 7000D mass spectrometer of Agilent Technologies) equipped with HP-5MS fused silica capillary columns (15 m × 0.25 mm × 0.25 µm). Carrier gas flow was 1 mL min⁻¹ in column 1 and 1.2 mL min⁻¹ in column 2. The GC oven temperature was programmed from 60 to 240 °C, at a rate of 3 °C min⁻¹. The injector temperature was set at 280 °C. The transfer line and source temperatures were set at 280 °C and 230 °C, respectively. The injection volume was 1.0 µL, with a split ratio of 30:1. Mass spectra were recorded in EI mode (70 eV), with a mass scan range from 50–500 amu. The identification of compounds was achieved based on retention time, mass spectral data, and mass spectral library search (MassHunter, NIST17.L). The external standards, including Eugenol (ACROS ORGANICS), Methyl eugenol (SIGMA-ALDRICH), Estragole (ACROS ORGANICS), Chavicol (MERCK), and Linalool (Thermo Scientific), were used for the identification of key compounds in the samples by comparing their mass spectra and retention times. The relative amounts of individual components in different samples were determined as peak area (%) from the total ion chromatogram (GC-MS).

2.4.3. Data Analysis

The Pearson correlation coefficient model in SPSS 20.0 (SPSS Inc., Chicago, IL, USA) was used to statistically analyse variations in the percentage composition of the volatile oil composition [71]. To determine similarities among the *O. basilicum* accessions, a UPGMA dendrogram was created. Additionally, using SPSS Statistics 20.0 software (SPSS Inc.), principal component analysis (PCA) was carried out utilising the percentage of essential oil constituents.

3. Results

Different tested samples were grown in a controlled environment and collected at the flowering stage. These samples were then analysed for genetic, chemical, and morphological variations to identify differences among the tested samples. These analyses are crucial for both scientific and industrial purposes.

3.1. Genetic Analysis

Four DNA barcode regions (*matK*, *trnH-psbA*, *rbcL* and *rpl16*) were selected and sequenced. Additionally, sequences for nine other *Ocimum* species were retrieved from NCBI (accession numbers listed in Table 3) to expand the scope of the analysis and support species-level differentiation within the genus. After cleaning and aligning the sequences using the CLC platform and MEGA11, high sequence similarity was observed among tested samples and reference sequences from NCBI, particularly in the *rbcL* and *rpl16* regions. However, our study does not support their utility in assessing genetic relationships within *Ocimum*. Phylogenetic analysis and single-nucleotide polymorphism (SNP) analysis were performed using the *matK* and *trnH-psbA* regions.

3.1.1. Phylogenetic Analysis

A Neighbour-Joining analysis was performed using 1000 bootstrap (BS) replicates in MEGA 11 to assess the phylogenetic relationships among the *Ocimum* species and tested samples. In the *matK* phylogenetic tree, the clades were poorly resolved compared to the *trnH-psbA* tree. The tested samples formed a separate clade with *O. basilicum*, its hybrids, and related species *O. americanum* L., *O. campechianum* Mill., and *O. kilimandscharicum* Gürke, though this grouping had a low BS value. In contrast, the *trnH-psbA* tree provided better resolution and higher BS support. In this tree, *O. tenuiflorum* Burm.f., *O. gratissimum* Forssk., *O. filamentosum* Forssk., and *O. campechianum* Mill. formed a distinct, well-supported clade (BS 95%), separated from the rest of the *Ocimum* species (Figure 1). The phylogenetic analysis indicated that the tested samples likely belong to *O. basilicum*, its hybrids, or distinct species. However, this inference lacks strong support due to the reliance on single-region phylogenetic trees.

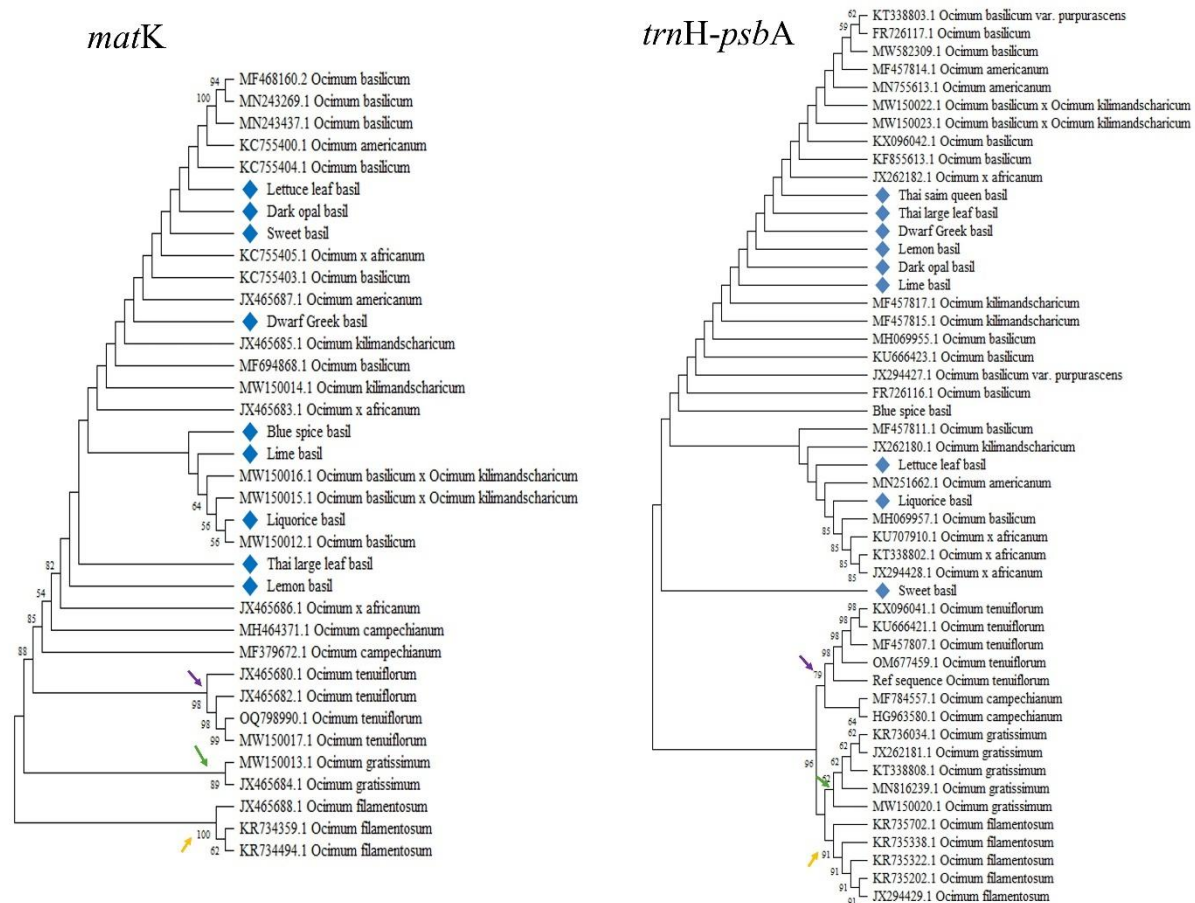


Figure 1. Phylogenetic trees reconstructed using neighbour-joining analysis based on the *matK* and *trnH-psbA* regions. BS values > 50% from 1000 replicates are indicated above the nodes. Blue symbols represent the tested samples, while arrow colours represent different species, with each species assigned a unique colour.

3.1.2. SNVs

To further investigate genetic variability, nucleotide variation analysis and the development of DNA barcodes were carried out. SNVs were detected in both *matK* and *trnH-psbA* regions, which enabled differentiation between certain *Ocimum* species and positioning of the tested basil samples. The *matK* analysis revealed species-specific variations across different regions (Figure 2). *O. filamentosum* showed distinct markers in Regions II, III, and IV. *O. gratissimum* displayed unique variations in Regions I and III. *O. tenuiflorum* was distinguished by variations in Regions II and III. Liquorice basil and *O. basilicum* × *O. kilimandscharicum* displayed similarity in their sequences within Region II, while showing variation from other species and samples.

The *trnH-psbA* region exhibited more considerable variation among *Ocimum* species (Figure 2). In the *trnH-psbA*-region I, variations were found to differentiate between *O. tenuiflorum*, *O. filamentosum*, and other species. However, a distinct sequence (*trnH-psbA*-II) with significant variations was identified across all nine *Ocimum* species. Due to the uniqueness of this sequence, it was designated as the “signature *trnH-psbA* sequence” for the genus *Ocimum* (Figure 2). This signature sequence in the *trnH-psbA* region serves as a valuable molecular marker for differentiating species within the genus. However, liquorice basil showed sequence similarity with *O. africanum*, and *O. basilicum* × *O. kilimandscharicum* displayed similarity with *O. americanum*, suggesting limitations in the marker’s ability to resolve these closely related accessions.

To address the sequence similarities observed in Figure 2 and avoid the need to test and sequence multiple barcoding regions, we designed a simple and effective two-step targeted approach. In the first step, the unique signature sequence in the *trnH-psbA* region can differentiate the majority of species and be sufficient to authenticate most of the accessions, as shown in Figure 2. This sequence allows the identification of *O. basilicum*, *O. gratissimum*, *O. tenuiflorum*, *O. filamentosum*, *O. campechianum*, *O. kilimandscharicum*. However, for species sharing identical sequences in this signature region, such as liquorice basil, genetically similar to *O. africanum*, and *O. basilicum* × *O. kilimandscharicum*, genetically similar to *O. americanum*, Step 2 is necessary. This step involves using the *matK* region II (Figures 2 and 3) to differentiate these species. *O. africanum* presents a single

nucleotide variation when compared to liquorice basil, and similarly, the same single nucleotide variation can differentiate *O. americanum* from *O. basilicum* × *O. kilimandscharicum*. Therefore, by combining both regions using this two-step approach, all species within *Ocimum* can be effectively differentiated. The two-step approach is outlined in Figure 3.

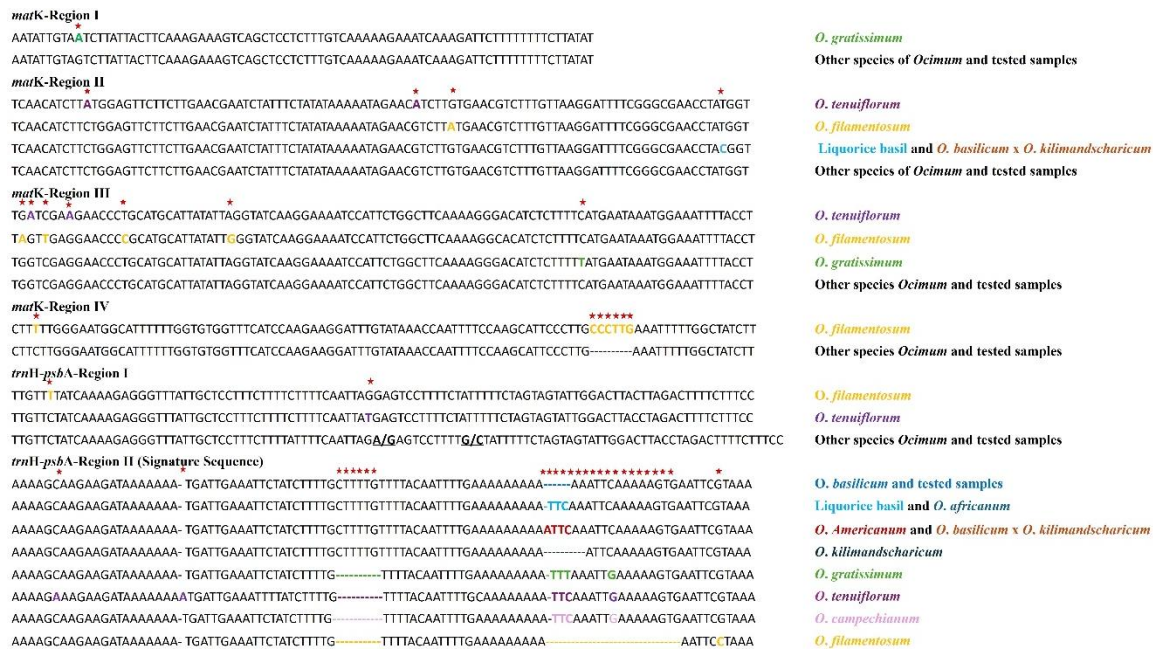


Figure 2. Sequence variations were manually constructed using the results of multiple alignments from MEGA11 for different varieties of *O. basilicum*, tested samples and species within the genus *Ocimum*. Different colours were assigned to each species for a clear distinction.

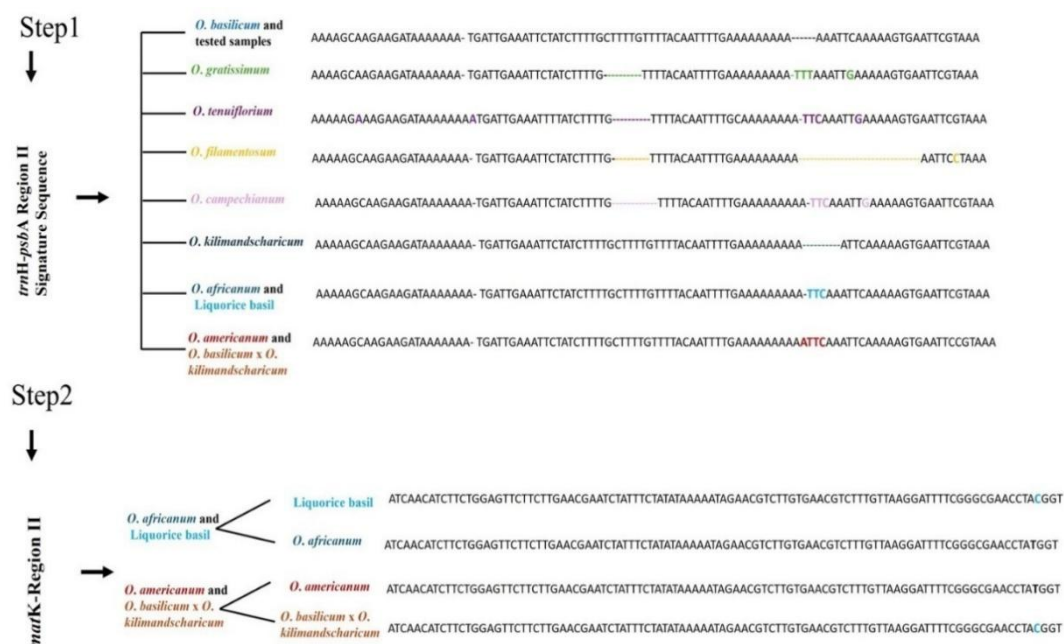


Figure 3. Diagrammatic representation of the strategy for differentiating various species of *Ocimum* and tested samples using DNA barcode regions.

In this study, hybrid species such as *O. basilicum* × *O. kilimandscharicum* and *O. africanum* exhibited sequence similarities with other taxa, complicating clear resolution and highlighting the limitations of the *trnH-psbA* marker in distinguishing hybrids. The integration of additional markers, such as *matK*, can enhance resolution and help address these challenges, enabling more accurate differentiation of hybrid species from other *Ocimum* taxa.

Following the two-step strategy outlined in this study, all commercial samples could be identified as *O. basilicum*. However, most labels correctly include the species name, aside from liquorice basil, which is labelled as *O. basilicum* but genetically aligns more closely with other *Ocimum* species. This suggests that its classification within *O. basilicum* needs to be reconsidered.

To explore the differences among the commercial samples that were not detected by the DNA approach, we sought to determine whether variations at the trichome and chemical levels could provide additional insights, explaining why these samples have been marketed under distinct names.

3.2. Micro-Morphological Analysis

In this study, our observations revealed that all samples contained glandular trichomes (GTs), both capitate, peltate, and non-glandular trichome (NTG), as shown in Figure 4. In the accessions where NGT were absent in the areas away from the midrib (Figure 4A), they were present in the midrib region (Figure 4B). This confirms that NGT was present in all accessions used in the study.

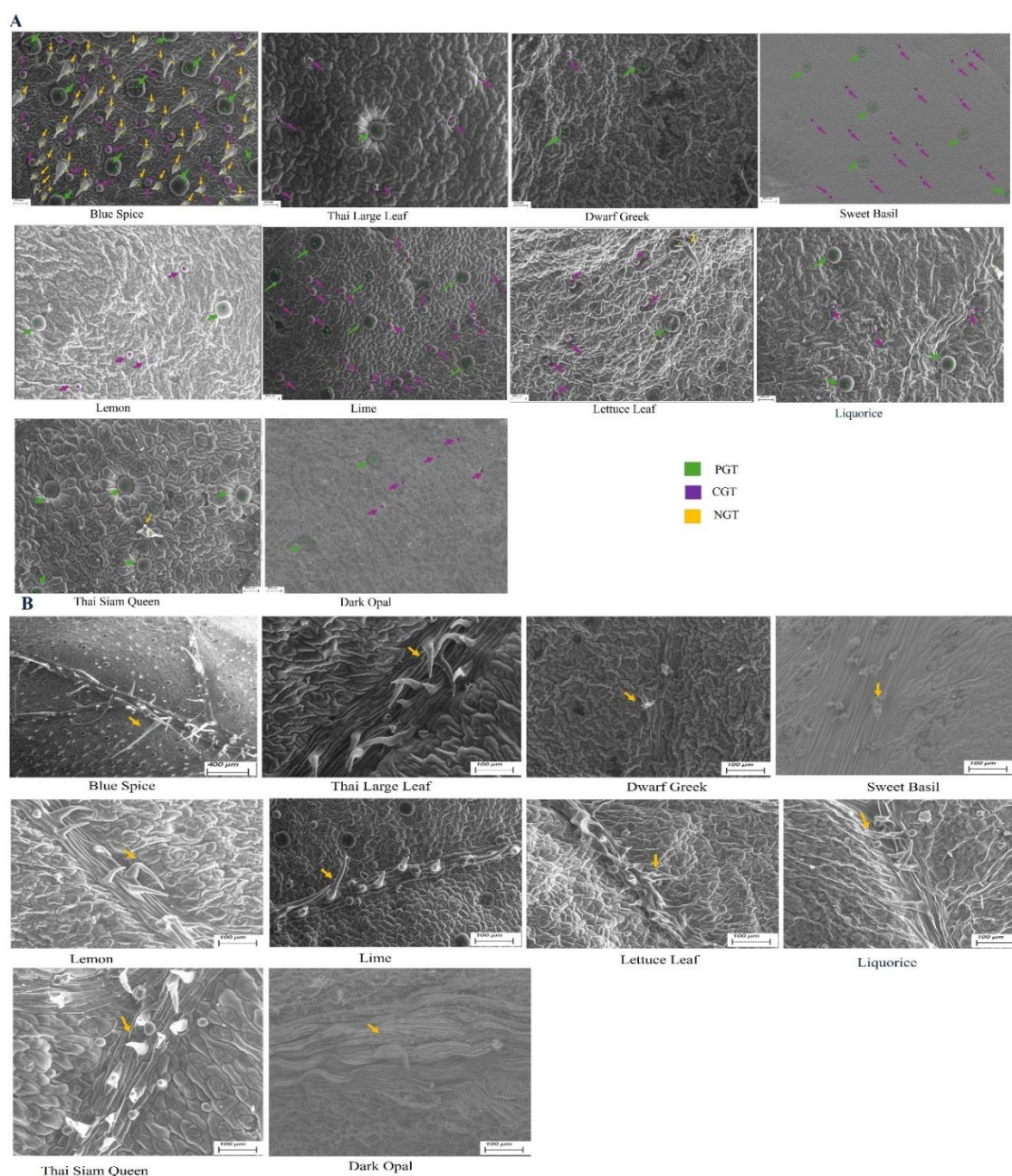


Figure 4. SEM images of foliar trichomes in *O. basilicum*, showing different trichome types and their distribution across various accessions. (A) Foliar areas away from the midrib, imaged at 200× magnification. (B) Midrib area exhibiting NGT at varying magnifications.

Significant variations were observed in the abundance of different trichomes among accessions, as highlighted in Figure 5. For density calculations, areas (per mm²) away from the midrib were used. The blue spice is particularly noteworthy for its significantly high abundance of all trichome types. In contrast, other cultivars exhibit a much lower abundance of NGT compared to GTs. However, no distinct morphological differences in trichomes were observed that could be used to reliably differentiate the samples. Therefore, we proceeded to the next approach—chemical analysis.

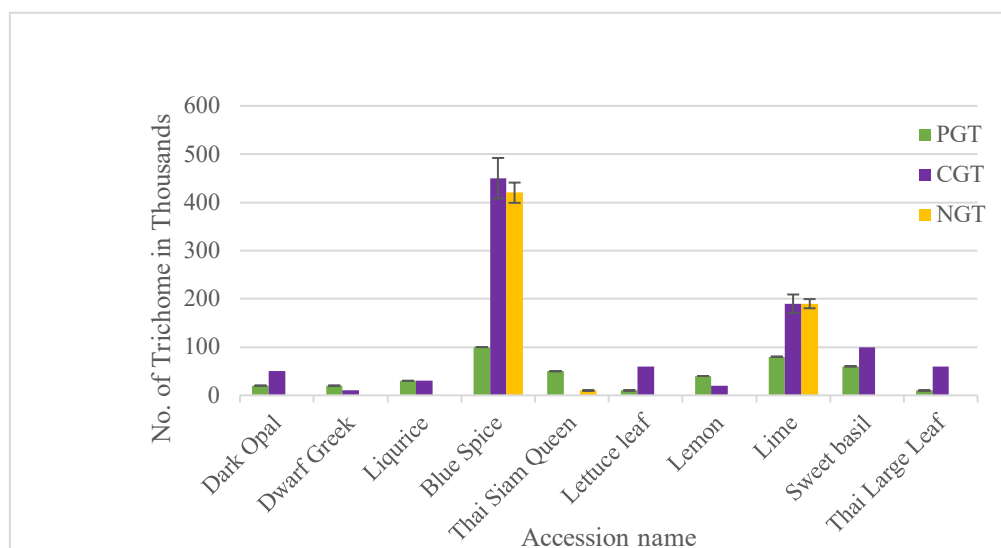


Figure 5. Trichome counting was performed on different samples using Fiji (ImageJ version 1.54f). The total number of trichomes per image (as shown in Figure 4A) was used to estimate trichome abundance. Error bars represent $\pm 10\%$ of the mean values, indicating the variability in measurements.

3.3. Chemical Analysis

A comprehensive analysis of essential oils from multiple basil accessions, using GC-MS, identified 31 distinct components (Table 4). The majority of samples (over 90%) were dominated by phenylpropenes, with concentrations ranging from 41.1% to 77.9%. The chemical composition of the tested basil accessions is summarised in Table 4, which provides peak area percentages of individual compounds. The results confirm the presence of key compounds such as linalool, methyl chavicol (estragole), methyl eugenol, and eugenol, reflecting the diversity in basil chemotypes. The grouping of samples based on their chemical profiles provides insight into the variability of key essential oil components across different tested samples (Figure 6A,B).

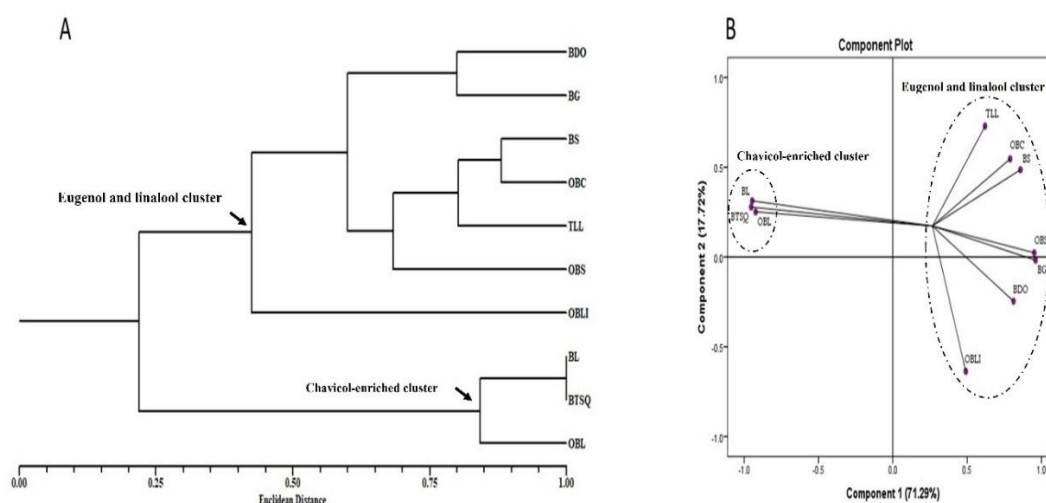


Figure 6. Hierarchical cluster analysis showing the chemical relationship among tested samples (A); PCA plot of the volatile oil components (B).

Table 4. Essential oil composition of tested samples. BDO = Dark Opal, BG = Dwarf Greek, BL = Liquorice Basil, BS = Blue Spice, BTSQ = Thai Siam Queen, OBC = Lettuce Leaf, OBL = Lemon, OBLI = Lime, OBS = Sweet Basil, TLL = Thai Large Leaf.

Compound	Peak Area (%)									
	BDO	BG	BL	BS	BTSQ	OBC	OBL	OBLI	OBS	TLL
α -Pinene	1.2	-	-	-	-	1.2	-	-	-	-
β -Pinene	1.7	-	1.0	-	-	1.9	-	-	1.2	-
Myrcene	1.9	-	-	-	-	-	-	-	1.1	-
1,8-Cineole	18.6	3.3	8.4	9.5	3.2	28.4	-	3.1	13.2	4.2
(<i>E</i>)- β -Ocimene	-	-	2.8	3.5	2.1	2.9	-	-	1.4	-
γ -Terpinene	-	-	-	-	-	-	-	1.9	-	-
Fenchone	1.7	-	-	-	-	-	0.8	-	-	-
Linalool	7.2	14.0	-	-	9.5	-	-	29.9	33.4	11.3
Camphor	1.8	-	1.6	-	-	-	-	-	-	-
Borneol	-	-	-	-	0.9	-	-	-	-	-
Terpinen-4-ol	-	2.8	-	-	-	-	-	6.0	-	4.4
α -Terpineol	-	-	-	-	-	-	-	-	-	0.7
Methyl chavicol *	-	-	77.6	11.0	69.6	17.3	56.4	-	-	31.6
Nerol	-	-	-	-	-	-	3.8	-	-	-
Neral (=citral b)	-	-	-	-	-	-	11.4	17.8	-	-
Chavicol	-	-	-	1.2	-	-	-	-	-	-
Geraniol	-	-	-	-	-	-	3.8	-	-	-
Geranial (=citral a)	-	-	-	-	-	-	13.5	21.1	-	-
Bornyl acetate	-	1.8	-	-	-	-	-	-	-	-
Eugenol	18.9	38.7	-	49.5	-	34.9	-	-	39.4	40.8
β -Elemene	-	4.9	1.5	-	0.7	-	-	-	1.6	-
Methyl eugenol	43.5	27.0	-	-	8.3	-	0.8	-	1.7	4.3
β -Caryophyllene	-	-	-	1.3	-	-	3.8	7.3	-	-
<i>trans</i> - α -Bergamotene	3.5	1.8	-	-	2.5	-	-	4.8	2.4	1.2
α -Humulene	-	-	-	1.4	-	-	-	-	-	-
Germacrene D	-	2.7	2.0	3.1	-	1.0	2.5	4.7	-	-
β -Bisabolene	-	-	-	9.6	-	6.6	-	-	-	-
α -Bulnesene	-	2.8	0.8	-	-	-	-	-	-	-
γ -Cadinene	-	-	1.2	-	1.0	-	-	-	-	0.5
α -Bisabolene	-	-	-	9.9	-	5.5	3.2	3.4	-	-
<i>epi</i> - α -Cadinol	-	-	3.1	-	2.1	-	-	-	4.6	1.0
Class composition	Peak Area (%)									
	BDO	BG	BL	BS	BTSQ	OBC	OBL	OBLI	OBS	TLL
<i>Monoterpenoids</i>										
Monoterpene hydrocarbons	4.8	-	3.8	3.5	2.1	6.0	-	1.9	3.7	-
Oxygenated monoterpenes	29.3	21.9	10.0	9.5	13.6	28.4	33.4	77.9	46.6	20.6
<i>Sesquiterpenoids</i>										
Sesquiterpene hydrocarbons	3.5	12.2	5.5	25.3	4.2	13.1	9.5	20.2	4.0	1.7
Oxygenated sesquiterpenes	-	-	3.1	-	2.1	-	-	-	4.6	1.0
<i>Phenylpropanoids</i>	62.4	65.7	77.6	61.7	77.9	52.2	57.2	-	41.1	76.7

* Methyl chavicol (=Estragole).

3.3.1. Eugenol and Linalool Cluster

Hierarchical clustering (Figure 6A,B) reveals distinct groupings based on essential oil composition. This group includes accessions such as Dark Opal, Dwarf Greek, Blue Spice, Lettuce Leaf, Thai Large Leaf, Sweet Basil, and Lime.

In this group, Thai Large Leaf accession showed relatively high concentrations of phenylpropene-type compounds (76.7%). The other accessions Dark Opal, Dwarf Greek, Lettuce Leaf, and Sweet Basil contained moderate amounts of both phenylpropenes (62.4%, 65.7%, 52.2%, and 41.1%, respectively) and oxygenated monoterpenes (29.3%, 21.9%, 28.4%, and 46.6%, respectively). Notably, Blue Spice contained the highest percentage of sesquiterpene hydrocarbons (25.3%), in addition to phenylpropenes (61.7%) and oxygenated monoterpenes (9.5%). This accession also exhibited a higher abundance of GTs, indicating a positive correlation between trichome density and the concentration of essential oil compounds.

A further breakdown shows that the concentration of eugenol or methyl eugenol in this group is significantly higher compared to the other cluster. For instance, the Dark Opal and Blue Spice accessions were dominated by

eugenol (49.5%) and methyl eugenol (43.5%), respectively, while the Thai Large Leaf also displayed moderate concentrations of both eugenol (40.8%) and methyl chavicol (31.6%). These findings suggest differential enzyme activity within the phenylpropanoid pathway (Figure 7).

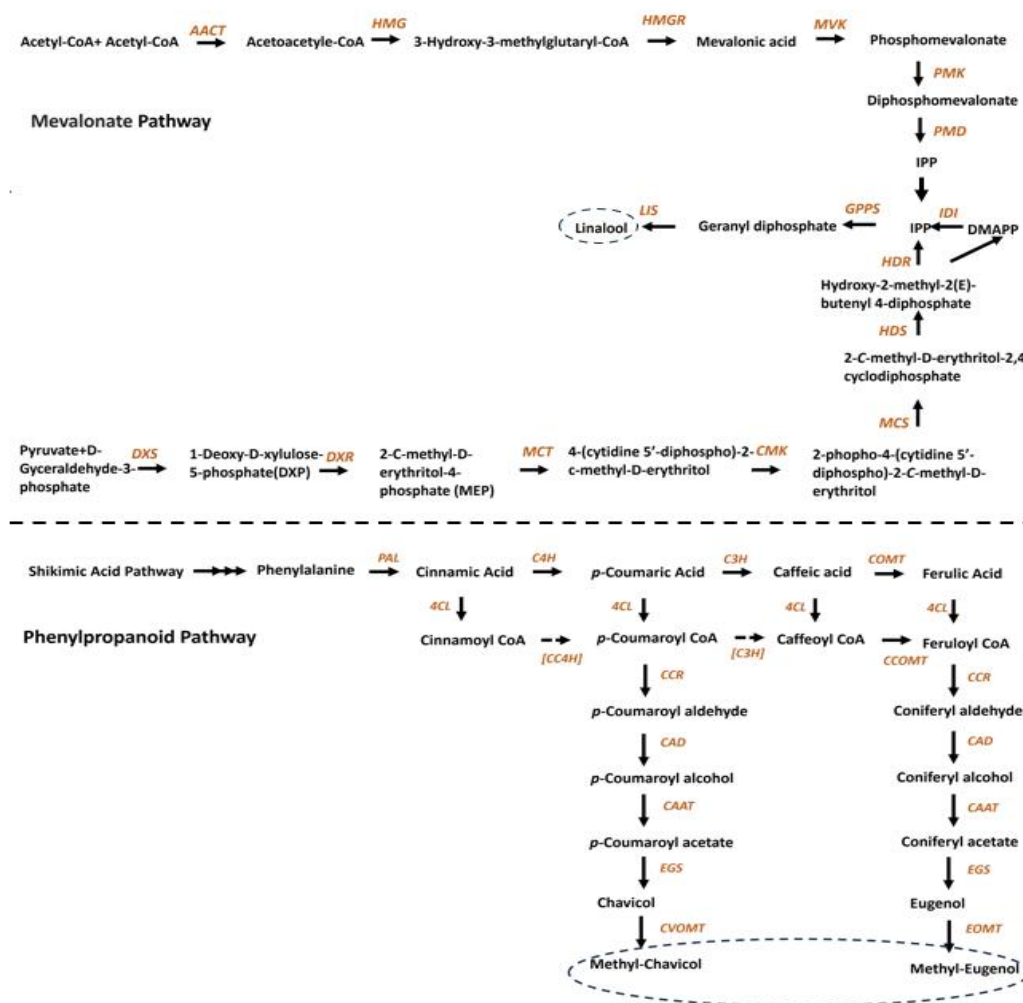


Figure 7. An overview of Mevalonate Pathway and phenylpropanoid pathways leading to the generation of linalool and methylate-phenylpropenes in *Ocimum basilicum*. DXS, DXP synthase; DXR, DXP reducto isomerase; MCT, 2-C-methyl-D-erythritol-4-(cytidyl-5-diphosphate) transferase; CMK, CDP-ME kinase; MCS, CMEPP synthase; HDS, HMBPP synthase; HDR, hydroxy-2-methyl-2(E)-butenyl 4-diphosphate reductase; IDI, IPP isomerase; AACT (acetoacetyl-CoA thiolase), HMGS (HMG synthase), HMGR (HMG reductase), MVK, MVA kinase; PMK, phosphome-valonate kinase; PMD, MVA diphosphate decarboxylase; GPPS, GGPP synthase, LIS, Linalool Synthase, PAL, phenylalanine ammonia lyase; C4H, cinnamate 4-hydroxylase; 4CL, 4-coumarate: CoA ligase; C3H, p-coumarate 3-hydroxylase; COMT, caffeoyl O-methyl transferase; CC4H, cinnamoyl-CoA 4-hydroxylase; CC3H, p-coumaroyl- CoA 3-hydroxylase; CCOMT, caffeoyl-CoA O-methyl transferase; CCR, cinnamoyl-CoA reductase; CAD, cinnamyl alcohol dehydrogenase; CAAT, coniferyl alcohol acetyl transferase; EGS, eugenol synthase; EOMT, eugenol O-methyl transferase and CVOMT, chavicol O-methyl transferase. The enzymes for 4- and 3-hydroxylation of CoA esters have not been demonstrated yet, and hence [CC4H] and [CC3H] are indicated in brackets to indicate their probable role (adapted from Rastogi et al. [62]).

Linalool, a desirable constituent known for its mild, floral fragrance, was found in moderate concentration in the accession Lime (29.9%) and Sweet Basil (33.4%). Lime also exhibited notable levels of citral (neral: 17.8%, geranial: 21.1%) while exhibiting minimal or no expression of eugenol, methyl eugenol, or methyl chavicol. Conversely, Sweet Basil displayed substantial eugenol content (39.4%).

Another observation in our findings was that all samples were collected for analysis during the flowering stage. The observed variability in the expression of compounds suggests that developmental stages play a significant role in determining the chemical profiles of a species.

3.3.2. Methyl Chavicol-Enriched Cluster

This cluster includes three accessions: Liquorice and Thai Siam Queen, which are highly enriched in methyl chavicol (77.6% and 69.6%, respectively), and Lemon, which contains methyl chavicol at a lower concentration (56.4%) along with significant amounts of citral (neral 11.4%, geranial 13.5%) (Figure 6A,B). The high concentration of methyl chavicol in these accessions differentiates them from others at the flowering stage. This suggests that chavicol (if harvested earlier) or methyl chavicol, in combination with the absence of eugenol or low levels methyl eugenol (<10%), could serve as effective chemical markers for identification of these samples. However, the reliability of these markers is highly dependent on the harvesting stage. In addition, the high concentration of methyl chavicol in Liquorice Basil suggests a closer relationship with *O. basilicum* than genetic analysis alone indicates. In genetic variation studies, Liquorice Basil exhibited similarities with other *Ocimum* species, highlighting a discrepancy between genetic and chemical classifications. This inconsistency complicates the authentication of Liquorice Basil as *O. basilicum*, as labelled on its packaging. Such discrepancies pose challenges for quality control processes.

4. Discussion

In the present study, multiple approaches were employed to differentiate commercial *O. basilicum* (basil) samples, including DNA barcoding, trichome analysis, and chemical profiling. The selected DNA barcode regions have been widely used and have demonstrated their effectiveness in distinguishing species within the genus *Ocimum* and related genera [21,40,42,54,61–63,72–79]. However, in our analysis, the phylogenetic resolution provided by these markers was limited. The phylogenetic trees based on the *trnH-psbA* and *matK* regions did not form a distinct clade for the *O. basilicum* samples, instead showing close genetic similarity with its hybrids, and failed to provide strong support for the monophyly of *O. basilicum*. In contrast, previous studies utilising complete chloroplast genome sequences have shown improved phylogenetic resolution within the genus [80,81]. These findings underscore the limitations of single regions and highlight the potential of whole-genome approaches for resolving complex taxonomic relationships within *Ocimum*.

DNA identification has proven to be a reliable method for species-level classification [82–85]. The *trnH-psbA* region in particular has been shown to be highly effective for species-level identification, including in the genus *Ocimum* [57,66,67,71,86–92]. It is also recognised by the British Pharmacopoeia as a DNA barcode for distinguishing *O. tenuiflorum* from other *Ocimum* species [86]. However, while DNA is effective at the species level, it is often insufficient for intraspecific identification due to the complexities introduced by selective breeding and hybridisation, particularly in commercially or ornamentally cultivated varieties [32,92–95]. Similarly, in this study, the DNA markers used were unable to distinguish *O. basilicum* from its hybrids. Although a two-step strategy was employed by incorporating an additional marker, these markers still failed to differentiate within the *O. basilicum* species. Basil commercial breeds have a long history of selective breeding and hybridisation, which can obscure genetic distinctions within the species. The use of universal DNA markers presents challenges in distinguishing varieties, cultivars, or chemotypes within the same species. To improve precision, it is necessary to develop specific DNA barcodes targeting chloroplast or nuclear genome sequences for more accurate identification. Since our focus was to discriminate between different forms of *O. basilicum*, DNA barcoding alone was not sufficient. Therefore, we proceeded to use morphological and chemical analyses to achieve better differentiation.

The presence of both GT and NGT is a common characteristic of plant species in the Lamiaceae family [96–101]. NGT plays a critical role in plant defence mechanisms, including reducing transpiration, enhancing tolerance to cold, deflecting intense solar radiation, and reducing herbivory [102–104]. GTs, on the other hand, serve as protective barriers against external stressors such as herbivores, pathogens, UV-B radiation, extreme temperatures, and drought through the volatile oils they secrete [104–107]. The presence of distinct trichome types also holds significant taxonomic value, offering potential markers for systematic studies within the Lamiaceae family [108–111]. In this study, our observations revealed that all samples contained capitate, peltate, and NTG trichome types, which are also found in other *Ocimum* species [112,113]. Trichome abundance can serve as a useful marker during the pre-processing stages. However, its utility diminishes once the sample has been processed [104,114]. Factors such as drying, mechanical handling, or prolonged storage may lead to the destruction or reduction of trichomes, as well as the evaporation of volatile compounds stored in glandular trichomes [115–118]. Moreover, the variability in trichome abundance between the midrib region and other leaf areas makes it less reliable for the authentication of processed samples. These changes can compromise the reliability of trichome-based assessments in processed samples [7,119]. Additionally, environmental factors play a significant role in the distribution and density of both GT and NGT. Variables such as light intensity, temperature, humidity, and soil conditions can influence trichome development, making it essential to account for these factors when assessing the quality of raw

materials [104,120,121]. Trichome morphology can offer valuable insights, especially in identifying plant species or verifying the presence of specific traits associated with bioactive compounds. However, relying solely on trichome abundance in basil accessions for quality assurance is proven insufficient [122,123]. Therefore, the study progressed to chemical analysis for more definitive differentiation.

Chemical analysis remains a valuable tool when assessing the presence of bioactive compounds, as DNA testing alone cannot confirm whether a compound is expressed. Here, chemical analysis revealed phenylpropenes as major constituents in basil essential oils, consistent with previous studies [45,124,125]. Hierarchical cluster analysis and PCA plots identified two major clusters: a eugenol and linalool-rich cluster and a chavicol-rich cluster. These results indicate variation in enzyme activity within the phenylpropanoid pathway. The substrate p-coumaroyl-CoA is predominantly directed towards conversion into caffeoyl-CoA, which serves as the substrate for eugenol biosynthesis rather than converting to p-coumaroyl aldehyde, which is subsequently directed towards the production of chavicol [61,126–128] (Figure 7). The enzyme eugenol O-methyltransferase catalyses the conversion of eugenol to methyl eugenol, and chavicol O-methyltransferase converts chavicol to methyl chavicol [129,130]. Eugenol is recognised as an allergenic compound [2,10], and both methyl eugenol and methyl chavicol have been implicated as potentially carcinogenic substances in prior studies [24,131–135]. This raises significant safety concerns, particularly given that certain accessions, such as Blue Spice and Dark Opal, exhibit high concentrations of these compounds. The observed variability in chemical profiles underscores the importance of carefully considering the biosynthetic pathways and their potential impact on the quality and safety of basil-derived products.

Linalool known for its mild, floral fragrance [136,137] was found in moderate concentration in the accession clustered in eugenol and linalool-rich cluster. In a study by Radulović et al. [138], α -linalool was proposed as a chemical marker for the authentication of *O. basilicum*, particularly in the accession of sweet basil. However, linalool concentrations as high as 94% have also been reported in other Lamiaceae members, such as *Mentha spicata*, which undermines its reliability as a species-specific marker for *O. basilicum* authentication [111]. Eugenol and methyl eugenol are two prominent constituents of basil essential oil; however, their concentrations are influenced by the developmental stage at harvest. Accessions showing high eugenol levels at the current stage may exhibit increased methyl eugenol concentrations if harvested later, as methyl eugenol is often biosynthesised from eugenol during maturation [135]. However, the reliability of chemical markers is influenced by the harvesting stage, as the concentration of secondary metabolites fluctuates throughout plant development [134,139–144]. If plants are not harvested at the optimal stage, variations in compound composition and quantity may affect the accuracy of chemical profiling. In addition, both eugenol and methyl eugenol are also major components of essential oils derived from *O. tenuiflorum*, making it challenging to consider these compounds as reliable chemical markers for the tested samples or other species within the *Ocimum* genus [89]. This limits their usefulness for classification or authentication within *O. basilicum*.

Methyl chavicol is widely used as a flavouring agent in the food industry and is approved by the Food and Drug Administration for such application [145]. However, it is considered an undesirable compound in essential oils due to potential health concerns [24,66]. The accessions in chavicol-rich cluster are aligned with the methyl chavicol-rich chemotype classification described by Lawrence et al. [49]. This suggests that chavicol (if harvested earlier) or methyl chavicol, in combination with the absence of eugenol or low levels methyl eugenol, could serve as effective chemical markers for identification of these samples. However, the reliability of these markers is highly dependent on the harvesting stage [140–144]. In addition, the high concentration of methyl chavicol in Liquorice Basil suggests a closer relationship with *O. basilicum* than genetic analysis alone indicates. In genetic variation studies, Liquorice Basil exhibited similarities with other *Ocimum* species, highlighting a discrepancy between genetic and chemical classifications. This inconsistency complicates the authentication of Liquorice Basil as *O. basilicum*, as labelled on its packaging. Such discrepancies pose challenges for quality control processes.

The choice of testing method should align with the research or industry objective. If the goal is species identification, DNA barcoding remains the most effective approach. However, if the objective is to verify compound composition and quality, chemical analysis is required. Our findings demonstrate that, although the majority of samples were identified as *O. basilicum*, their chemical profiles varied significantly. This highlights the need of a multi-tiered analytical approach—integrating both genetic and chemical assessments—to ensure the quality, authenticity, and safety of commercial basil products in quality control and authentication processes. This aligns with findings from other studies [39,53,55–58,146–151].

To improve industry standards, a multi-method authentication strategy should be adopted. This approach ensures a more robust and reliable means of verifying plant identity and product quality. Additionally, product labelling should provide comprehensive and accurate information, including the species name, variety, cultivar, and chemotype. This is particularly crucial for plant species that have undergone breeding or hybridisation for commercial

use. This comprehensive approach benefits the industry by mitigating risks associated with mislabelling and adulteration, while consumers gain confidence in the authenticity and quality of the products they purchase.

Author Contributions

N.N.: conceptualization, methodology, data curation, formal analysis, investigation, validation, visualization, writing—original draft preparation, reviewing, and editing; V.S.: methodology, data curation, formal analysis, reviewing, and editing; R.S.V.: analysis, reviewing, and editing; A.S.: supervision, reviewing, and editing; R.A.: supervision, resources, methodology, data curation, and editing; T.S.: supervision, resources, methodology, data curation, reviewing and editing, funding acquisition, and project administration. All authors have read and agreed to the published version of the manuscript.

Funding

This research was funded by the Biotechnology and Biological Sciences Research Council (BBSRC) and the Daphne Jackson Trust, UK, as well as by the Council of Scientific and Industrial Research (CSIR), India.

Institutional Review Board Statement

Not applicable.

Informed Consent Statement

Not applicable.

Data Availability Statement

All relevant data generated or analysed during this study are included in the figures and DNA sequences generated have been deposited in NCBI. The accession numbers for the DNA sequences are provided in the manuscript.

Acknowledgments

We would like to express our sincere appreciation to the BBSRC and the Daphne Jackson Trust for their invaluable financial support, which was instrumental in facilitating the completion of this research. Their contribution has been crucial in enabling the successful execution of this study, and we are deeply grateful for their commitment to advancing scientific research. VS is thankful to CSIR, India, for awarding the Raman Research Fellowship to carry out this work as a part of his study at the Biomolecular Technology Group, Leicester School of Allied Health Science, Faculty of Health and Life Sciences, De Montfort University, Leicester, UK.

Conflicts of Interest

The authors declare no conflict of interest.

Use of AI and AI-Assisted Technologies

No AI tools were used in the preparation of this paper.

References

1. World Health Organization (WHO). *National Policy on Traditional Medicine and Regulation of Herbal Medicines: Report of a WHO Global Survey*; WHO: Geneva, Switzerland, 2005.
2. Conboy, L.; Kaptchuk, T.J.; Eisenberg, D.M.; et al. The relationship between social factors and attitudes toward conventional and CAM practitioners. *Complement. Ther. Clin. Pract.* **2007**, *13*, 146–157.
3. Rishton, G.M. Natural products as a robust source of new drugs and drug leads: Past successes and present-day issues. *Am. J. Cardiol.* **2008**, *101*, S43–S49.
4. Schmidt, B.; Ribnický, D.M.; Poulev, A.; et al. A natural history of botanical therapeutics. *Metabolism* **2008**, *57*, S3–S9.
5. Wachtel-Galor, S.; Benzie, I.F.F. Herbal Medicine: An Introduction to Its History, Usage, Regulation, Current Trends, and Research Needs. In *Herbal Medicine: Biomolecular and Clinical Aspects*, 2nd ed.; Benzie, I.F.F., Wachtel-Galor, S., Eds.; CRC Press/Taylor & Francis: Boca Raton, FL, USA, 2011.

6. Mendes, A.; Oliveira, A.; Lameiras, J.; et al. Organic Medicinal and Aromatic Plants: Consumption Profile of a Portuguese Consumer Sample. *Foods* **2023**, *12*, 4145.
7. Nazar, N.; Saxena, A.; Sebastian, A.; et al. Integrating DNA Barcoding Within an Orthogonal Approach for Herbal Product Authentication: A Narrative Review. *Phytochem. Anal.* **2025**, *36*, 7–29.
8. Theodoridis, S.; Drakou, E.G.; Hickler T.; et al. Evaluating natural medicinal resources and their exposure to global change. *Lancet Planet. Health* **2023**, *7*, e155–e163.
9. Li, Y.; Kong, D.; Fu, Y.; et al. The effect of developmental and environmental factors on secondary metabolites in medicinal plants. *Plant Physiol. Biochem.* **2020**, *148*, 80–89.
10. Ciocan, A.-G.; Tecuceanu, V.; Enache-Preoteasa, C.; et al. Phenological and Environmental Factors' Impact on Secondary Metabolites in Medicinal Plant *Cotinus coggygria* Scop. *Plants* **2023**, *12*, 1762.
11. Elshafie, H.S.; Camele, I.; Mohamed, A.A. A Comprehensive Review on the Biological, Agricultural and Pharmaceutical Properties of Secondary Metabolites Based-Plant Origin. *Int. J. Mol. Sci.* **2023**, *24*, 3266.
12. Chele, K.H.; Piater, L.A.; van der Hooft, J.J.J.; et al. Bridging Ethnobotanical Knowledge and Multi-Omics Approaches for Plant-Derived Natural Product Discovery. *Metabolites* **2025**, *15*, 362.
13. Chrysargyris, A.; Skaltsa, H.; Konstantopoulou, M. Medicinal and Aromatic Plants (MAPs): The Connection between Cultivation Practices and Biological Properties. *Agronomy* **2022**, *12*, 3108.
14. Vaou, N.; Voidarou, C.; Rozos, G.; et al. Unraveling Nature's Pharmacy: Transforming Medicinal Plants into Modern Therapeutic Agents. *Pharmaceutics* **2025**, *17*, 754.
15. Paz Arraiza, M.; Calderón-Guerrero, C.; Guillén, S.C.; et al. Industrial Uses of MAPs: The Pharmaceutical Sector. In *Medicinal and Aromatic Plants: The Basics of Industrial Application*; Paz-Arraiza, M., González-Coloma, A., Burilo, J., et al., Eds.; Bentham Science: Singapore, 2017; pp. 60–75.
16. Wang, H.; Chen, Y.; Wang, L.; et al. Advancing herbal medicine: Enhancing product quality and safety through robust quality control practices. *Front. Pharmacol.* **2023**, *14*, 1265178.
17. Balkrishna, A.; Sharma, N.; Srivastava, D.; et al. Exploring the Safety, Efficacy, and Bioactivity of Herbal Medicines: Bridging Traditional Wisdom and Modern Science in Healthcare. *Futur. Integr. Med.* **2024**, *3*, 35–49.
18. Wäldchen, J.; Rzanny, M.; Seeland, M.; et al. Automated plant species identification-Trends and future directions. *PLoS Comput. Biol.* **2018**, *14*, e1005993.
19. Pratiwi, R.; Dipadharma, R.H.F.; Prayugo, I.J.; et al. Recent Analytical Method for Detection of Chemical Adulterants in Herbal Medicine. *Molecules* **2021**, *26*, 6606.
20. Ichim, M.C. The DNA-Based Authentication of Commercial Herbal Products Reveals Their Globally Widespread Adulteration. *Front. Pharmacol.* **2019**, *10*, 1227.
21. Sgamma, T.; Lockie-Williams, C.; Kreuzer, M.; et al. DNA Barcoding for Industrial Quality Assurance. *Planta Med.* **2017**, *83*, 1117–1129.
22. Pant, P.; Pandey, S.; Dall'Acqua, S. The Influence of Environmental Conditions on Secondary Metabolites in Medicinal Plants: A Literature Review. *Chem. Biodivers.* **2021**, *18*, e2100345.
23. Dong, P.; Wang, L.; Qiu, D.; et al. Evaluation of the environmental factors influencing the quality of *Astragalus membranaceus* var. *mongholicus* based on HPLC and the Maxent model. *BMC Plant Biol.* **2024**, *24*, 697.
24. International Fragrance Association (IFRA). IFRA Code of Practice. Available online: <https://ifrafragrance.org/initiatives-positions/safe-use-fragrance-science/ifra-standards/ifra-code-of-practice> (accessed on 13 July 2025).
25. Perfumer & Flavorist. Special Report: 26th Meeting of the ISO/TC54 Committee for the Standardization of Essential Oils. Available online: <https://www.perfumerflavorist.com/fragrance/regulatory-research/news/21884333/special-report-26th-meeting-of-the-iso-tc54-committee-for-the-standardization-of-essential-oils> (accessed on 24 July 2025).
26. European Directorate for the Quality of Medicines & HealthCare (EDQM). Content of the Dossier for Herbal Drugs and Herbal Drug Preparations—Quality Evaluation. Available online: https://www.edqm.eu/documents/52006/66253/Content%2Bof%2Bthe%2BDossier%2Bfor%2BHerbal%2BDrugs%2BAnd%2BHerbal%2BDrug%2BPreparation%2BQuality%2BEvaluation%2B%28PA_PH_CEP%2B%2802%29%2B6%2B1R%2C%2BFebruary%2B2013%29.pdf/3aeab5e-0a5b-2578-61fd-c2a3f8a99cb3 (accessed on 24 July 2025).
27. Booker, A.; Agapouda, A.; Frommenwiler, D.A.; et al. St John's wort (*Hypericum perforatum*) products—An assessment of their authenticity and quality. *Phytomedicine* **2018**, *40*, 158–164.
28. Manayi, A.; Vazirian, M.; Saeidnia, S. *Echinacea purpurea*: Pharmacology, phytochemistry and analysis methods. *Pharmacogn. Rev.* **2015**, *9*, 63–72.
29. Mahgoub, Y.A.; Shawky, E.; Eldakak, M.; et al. Plant DNA Barcoding and Metabolomics for Comprehensive Discrimination of German Chamomile from Its Poisonous Adulterants for Food Safety. *Food Control* **2022**, *136*, 108840.
30. Allkin, B. Useful Plants—Medicines: At Least 28,187 Plant Species Are Currently Recorded as Being of Medicinal Use. In *State of the World's Plants 2017*; Willis, K.J., Ed.; Royal Botanic Gardens Kew: London, UK, 2017.

31. Grayer, R.J.; Kite, G.C.; Goldstone, F.J.; et al. Intraspecific taxonomy and essential oil chemotypes in sweet basil, *Ocimum basilicum*. *Phytochemistry*. **1996**, *43*, 1033–1039.
32. Nazar, N.; Howard, C.; Slater, A.; et al. Challenges in Medicinal and Aromatic Plants DNA Barcoding—Lessons from the Lamiaceae. *Plants* **2022**, *11*, 137.
33. da Silva, L.R.R.; Ferreira, O.O.; Cruz, J.N.; et al. *Lamiaceae* Essential Oils, Phytochemical Profile, Antioxidant, and Biological Activities. *Evid. Based Complement. Altern. Med.* **2021**, *2021*, 6748052.
34. Azizah, N.S.; Irawan, B.; Kusmoro, J.; et al. Sweet Basil (*Ocimum basilicum* L.)—A Review of Its Botany, Phytochemistry, Pharmacological Activities, and Biotechnological Development. *Plants* **2023**, *12*, 4148.
35. Kamelnia, E.; Mohebbati, R.; Kamelnia, R.; et al. Anti-inflammatory, immunomodulatory and anti-oxidant effects of *Ocimum basilicum* L. and its main constituents: A review. *Iran. J. Basic. Med. Sci.* **2023**, *26*, 617–627.
36. Transparency Market Research. Basil Essential Oil Market report. Available online: <https://www.transparencymarketresearch.com/basil-essential-oil-market.html> (accessed on 6 July 2025).
37. Helen, H. Investigation of the Cultivars of the Basil (*Ocimum*). *Econ. Bot.* **1974**, *28*, 63–67.
38. Roberto, F.V.; Simon, J.E. Chemical Characterization of Basil (*Ocimum* spp.) Found in the Markets and Used in Traditional Medicine in Brazil. *Econ. Bot.* **2000**, *54*, 207–216.
39. Padalia, R.C.; Verma, R.S.; Chauhan, A. Analyses of organ specific variations in essential oils of four *Ocimum* species. *J. Essent. Oil Res.* **2014**, *26*, 409–419.
40. Svedman, C.; Engfeldt, M.; Api, A.M.; et al. Does the new standard for eugenol designed to protect against contact sensitization protect those sensitized from elicitation of the reaction? *Dermatitis* **2012**, *23*, 32–38.
41. International Fragrance Association (IFRA); Research Institute for Fragrance Materials (RIFM). IFRA RIFM QRA Information Booklet, Version 7.1; Revised July 9, 2015. Available online: <https://ifrafragrance.org> (accessed on 9 July 2025).
42. Ofenloch, R.F.; Andersen, K.E.; Foti, C.; et al. Allergic reactivity for different dilutions of eugenol in repeated open application test and patch testing. *Contact Dermat.* **2023**, *89*, 95–102.
43. Mulugeta, S.M.; Pluhár, Z.; Radácsi, P. Phenotypic Variations and Bioactive Constituents among Selected *Ocimum* Species. *Plants* **2024**, *13*, 64.
44. Srivastava, A.; Gupta, A.; Sarkar, S.; et al. Genetic and chemotypic variability in basil (*Ocimum basilicum* L.) germplasm towards future exploitation. *Ind. Crops Prod.* **2018**, *112*, 815–820.
45. Varga, F.; Carović-Stanko, K.; Ristić, M.; et al. Morphological and biochemical intraspecific characterization of *Ocimum basilicum* L. *Ind. Crops V. Prod.* **2017**, *109*, 611–618.
46. Avetisyan, A.; Markosian, A.; Petrosyan, M. et al. Chemical composition and some biological activities of the essential oils from basil *Ocimum* different cultivars. *BMC Complement. Altern. Med.* **2017**, *17*, 60.
47. Carović-Stanko, K.; Ribić, A.; Grdiša, M.; et al. Identification and discrimination of *Ocimum basilicum* L. morphotypes. In Proceedings of the 46th Croatian and 6th International Symposium on Agriculture, Opatija, Croatia, 14–18 February 2011.
48. Juškevičienė, D.; Radzevičius, A.; Viškelis, P.; et al. Estimation of Morphological Features and Essential Oil Content of Basils (*Ocimum basilicum* L.) Grown under Different Conditions. *Plants* **2022**, *11*, 1896.
49. Lawrence, B.M. A further examination of the variation of *Ocimum basilicum* L. In *Flavors and Fragrances: A World Perspective*; Lawrence, B.M., Mookerjee, B.D., Willis, B.J., Eds.; Elsevier Science Publishers B.V: Amsterdam, The Netherlands, 1988; pp. 161–170.
50. Muráriková, A.; Ťažký, A.; Neugebauerová, J.; et al. Characterization of Essential Oil Composition in Different Basil Species and Pot Cultures by a GC-MS Method. *Molecules* **2017**, *22*, 1221.
51. Gurav, T.P.; Dholakia, B.B.; Giri, A.P. A glance at the chemodiversity of *Ocimum* species: Trends, implications, and strategies for the quality and yield improvement of essential oil. *Phytochem. Rev.* **2022**, *21*, 879–913.
52. Padalia, R.C.; Verma, R.S.; Chauhan, A. Diurnal variations in aroma profile of *Ocimum basilicum* L., *O. gratissimum* L., *O. americanum* L., and *O. kilimandscharicum* Guerke. *J. Essent. Oil Res.* **2017**, *29*, 248–261.
53. Maggio, A.; Roscigno, G.; Bruno, M.; et al. Essential-Oil Variability in a Collection of *Ocimum basilicum* L. (Basil) Cultivars. *Chem. Biodivers.* **2016**, *13*, 1357–1368.
54. Ciriello, M.; Cirillo, V.; Formisano, L.; et al. Productive, Morpho-Physiological, and Postharvest Performance of Six Basil Types Grown in a Floating Raft System: A Comparative Study. *Plants* **2023**, *12*, 486.
55. Rusu, T.; Cowden, R.J.; Moraru, P.I.; et al. Overview of Multiple Applications of Basil Species and Cultivars and the Effects of Production Environmental Parameters on Yields and Secondary Metabolites in Hydroponic Systems. *Sustainability* **2021**, *13*, 11332.
56. Bazzicalupo, M.; Betuzzi, F.; Frigerio, J.; et al. Characterization of the floral traits, pollen micromorphology and DNA barcoding of the edible flowers from three basil taxa (Lamiaceae). *Genet. Resour. Crop Evol.* **2024**, *72*, 3383–3403.
57. Kumar, A.; Rodrigues, V.; Saxena, A.; et al. Evaluation of the plastid and nuclear DNA barcodes in the genus *Ocimum* towards quality assurance in the herbal industry. *Ind. Crops Prod.* **2025**, *224*, 120399.

58. Raclariu-Manolică, A.C.; Anmarkrud, J.A.; Kierczak, M.; et al. DNA Metabarcoding for Quality Control of Basil, Oregano, and Paprika. *Front. Plant Sci.* **2021**, *12*, 665618.
59. Mattia, F.D.; Bruni, I.; Galimberti, A.; et al. A comparative study of different DNA barcoding markers for the identification of some members of Lamiaceae. *Food Res. Int.* **2011**, *44*, 693–702.
60. Venkatesan, A.; Balaji, R.; Tanuja.; et al. Chloroplast genome of *Ocimum basilicum* var. *purpurascens* Benth 1830 (Lamiaceae). *Mitochondrial DNA B Resour.* **2024**, *9*, 252–256.
61. Rastogi, S.; Meena, S.; Bhattacharya, A.; et al. De novo sequencing and comparative analysis of holy and sweet basil transcriptomes. *BMC Genom.* **2014**, *15*, 588.
62. Gonda, I.; Faigenboim, A.; Adler, C.; et al. The genome sequence of tetraploid sweet basil, *Ocimum basilicum* L., provides tools for advanced genome editing and molecular breeding. *DNA Res.* **2020**, *27*, dsaa027.
63. Teliban, G-C.; Burducea, M.; Mihalache, G.; et al. Morphological, Physiological and Quality Performances of Basil Cultivars under Different Fertilization Types. *Agronomy* **2022**, *12*, 3219.
64. Varani, J.; Perone, P.; Spahlinger, D.M.; et al. Human skin in organ culture and human skin cells (keratinocytes and fibroblasts) in monolayer culture for assessment of chemically induced skin damage. *Toxicol. Pathol.* **2007**, *35*, 693–701.
65. de Araújo-Lopes, A.; da Fonseca, F.N.; Rocha, T.M.; et al. Eugenol as a Promising Molecule for the Treatment of Dermatitis: Antioxidant and Anti-inflammatory Activities and Its Nanoformulation. *Oxid. Med. Cell Longev.* **2018**, *2018*, 194849.
66. Bhamra, S.K.; Heinrich, M.; Johnson, M.R.D.; et al. The Cultural and Commercial Value of Tulsi (*Ocimum tenuiflorum* L.): Multidisciplinary Approaches Focusing on Species Authentication. *Plants* **2022**, *11*, 3160.
67. Maddi, R.; Amani, P.; Bhavitha, S.; et al. A review on *Ocimum* species: *Ocimum americanum* L., *Ocimum basilicum* L., *Ocimum gratissimum* L. and *Ocimum tenuiflorum* L. *Int. J. Res. Ayurveda Pharm.* **2019**, *10*, 41–48.
68. Jordan, W.C.; Courtney, M.W.; Neigel, J.E. Low levels of intraspecific genetic variation at a rapidly evolving chloroplast DNA locus in north American duckweeds (Lemnaceae). *Am. J. Bot.* **1996**, *83*, 430–439.
69. QIAGEN Bioinformatics. CLC Main Workbench. Available online: <https://www.qiagenbioinformatics.com/products/clc-main-workbench/> (accessed on 17 March 2025).
70. Tamura, K.; Stecher, G.; Kumar, S. MEGA 11: Molecular Evolutionary Genetics Analysis Version 11. *Mol. Bio Evol.* **2021**, *38*, 3022–3027.
71. Kumar, A.; Mishra, P.; Rodrigues, V.; et al. Delineation of *Ocimum gratissimum* L. complex combining morphological, molecular and essential oils analysis. *Ind. Crops Prod.* **2019**, *139*, 111536.
72. Partovi, R.; Iranbakhsh, A.; Sheidai, M.; et al. The use of DNA barcoding to avoid adulteration in olive plant leaf products. *Asian J. For.* **2021**, *5*. <https://doi.org/10.13057/asianjfor/r050106>.
73. Ekor, M. The growing use of herbal medicines: Issues relating to adverse reactions and challenges in monitoring safety. *Front. Pharmacol.* **2014**, *4*, 177.
74. Chase, M.W.; Salamin, N.; Wilkinson, M.; et al. Land plants and DNA barcodes: Short-term and long-term goals. *Philos. Trans. R. Soc. B* **2005**, *360*, 1889–1895.
75. Jürges, G.; Beyerle, K.; Tossenberger, M.; et al. Development and validation of microscopical diagnostics for ‘Tulsi’ (*Ocimum tenuiflorum* L.) in Ayurvedic preparations. *Eur. Food Res. Technol.* **2009**, *229*, 99–106.
76. Zhang, S.Y.; Yan, H.F.; Wei, L.; et al. Plastid genome and its phylogenetic implications of Asiatic *Spiraea* (Rosaceae). *BMC Plant Biol.* **2024**, *24*, 23.
77. Awad, M.; Fahmy, R.M.; Mosa, K.A.; et al. Identification of effective DNA barcodes for Triticum plants through chloroplast genome-wide analysis. *Comput. Biol. Chem.* **2017**, *71*, 20–31.
78. Qian, Z.H.; Munywoki, J.M.; Wang, Q.F.; et al. Molecular Identification of African *Nymphaea* Species (Water Lily) Based on ITS, *trnT-trnF* and *rpl16*. *Plants* **2022**, *11*, 2431.
79. Wang, A.K.; Lu, Q.F.; Zhu, Z.X.; et al. Exploring phylogenetic relationships within the subgenera of *Bambusa* based on DNA barcodes and morphological characteristics. *Sci. Rep.* **2022**, *12*, 8018.
80. Yesuthason, R.S.; Balaji, R.; Tanuja, P.M. The complete chloroplast genome and phylogenetic analysis of *Ocimum kilimandscharicum* Gurke (Camphor Basil) from India. *Mitochondrial DNA B Resour.* **2021**, *6*, 2164–2165.
81. Balaji, R.; Ravichandiran, K.; Tanuja, P.M. The complete chloroplast genome of *Ocimum gratissimum* from India—A medicinal plant in the Lamiaceae. *Mitochondrial DNA B Resour.* **2021**, *6*, 948–950.
82. Wong, K.H.; Zheng, T.; Yue, G.G. et al. A Systematic Approach for Authentication of Medicinal *Patrinia* Species Using an Integration of Morphological, Chemical and Molecular Methods. *Sci. Rep.* **2024**, *14*, 6566.
83. de Vere, N.; Rich, T.C.; Trinder, S.A.; et al. DNA barcoding for plants. *Methods Mol. Biol.* **2015**, *1245*, 101–118.
84. Letsiou, S.; Madesis, P.; Vasdekis, E.; et al. DNA Barcoding as a Plant Identification Method. *Appl. Sci.* **2024**, *14*, 1415.
85. Li, H.; Xiao, W.; Tong, T.; et al. The specific DNA barcodes based on chloroplast genes for species identification of Orchidaceae plants. *Sci. Rep.* **2021**, *11*, 1424.
86. British Pharmacopoeia. SC VII D. DNA Barcoding as a Tool for Botanical Identification of Herbal Drugs. Available online:

- https://www.google.com/url?sa=t&source=web&rct=j&opi=89978449&url=https://www.pharmacopoeia.com/bp-2021/supplementary-chapters/sc-7/sc-vii-d--dna-barcoding-as-a-tool-for-botanical-identification-o.html%3Fdate%3D2021-07-01%26text%3DDNA&ved=2ahUKEwiEhOOjurKQAxXjmokEHdsRKYsQFnoECAgQAQ&authuser=1&usq=AOvVaw1AOtoGeRblx9bB-FkLBYw_ (accessed on 17 March 2025)
87. Christina, V.L.; Annamalai, A. Nucleotide based validation of *Ocimum* species by evaluating three candidate barcodes of the chloroplast region. *Mol. Ecol. Resour.* **2014**, *14*, 60–68.
 88. Wu, H.-Y.; Shaw, P.-C. Strategies for Molecular Authentication of Herbal Products: From Experimental Design to Data Analysis. *Chin. Med.* **2022**, *17*, 38.
 89. Jorges, G.; Sahi, V.; Rodriguez, D.R.; et al. Product authenticity versus globalisation—The Tulsi case. *PLoS ONE* **2018**, *13*, e0207763.
 90. Loera-Sánchez, M.; Studer, B.; Kölliker, R. DNA barcode *trnH-psbA* is a promising candidate for efficient identification of forage legumes and grasses. *BMC Res. Notes* **2020**, *13*, 35.
 91. Frigerio, J.; Agostinetti, G.; Mezzasalma, V.; et al. DNA-Based Herbal Teas' Authentication: An ITS2 and *psbA-trnH* Multi-Marker DNA Metabarcoding Approach. *Plants* **2021**, *10*, 2120.
 92. Besse, P.; Da Silva, D.; Grisoni, M. Plant DNA Barcoding Principles and Limits: A Case Study in the Genus *Vanilla*. *Methods Mol. Biol.* **2021**, *2222*, 131–148.
 93. Zhang, W.; Sun, Y.; Liu, J.; et al. DNA barcoding of *Oryza*: Conventional, specific, and super barcodes. *Plant Mol. Biol.* **2021**, *105*, 215–228.
 94. Chen, S.; Yin, X.; Han, J.; et al. DNA barcoding in herbal medicine: Retrospective and prospective. *J. Pharm. Anal.* **2023**, *13*, 431–441.
 95. Samarina, L.S.; Koninskaya, N.G.; Shkhalakhova, R.M.; et al. DNA-Barcoding for Cultivar Identification and Intraspecific Diversity Analysis of Agricultural Crops. *Int. J. Mol. Sci.* **2025**, *26*, 6808.
 96. Huang, S.; Kirchoff, B.K.; Liao, J. The Capitate and Peltate Glandular Trichomes of *Lavandula pinnata* L. (Lamiaceae): Histochemistry, Ultrastructure, and Secretion. *J. Torrey Bot. Soc.* **2008**, *135*, 155–167.
 97. Santos, T.L.R.D.; De Melo, S.S.C.; Rodrigues, T.M. Non-Glandular Trichomes in Lamiaceae and Verbenaceae Species: Morphological and Histochemical Features Indicate More than Physical Protection. *N. Z. J. Bot.* **2016**, *54*, 446–457.
 98. Gostin, I.N. Glandular and Non-Glandular Trichomes from *Phlomis herba-venti* subsp. *pungens* Leaves: Light, Confocal, and Scanning Electron Microscopy and Histochemistry of the Secretory Products. *Plants* **2023**, *12*, 2423.
 99. Serrato-Valenti, G.; Bisio, A.; Cornara, L.; et al. Structural and histochemical investigation of the glandular trichomes of *Salvia aurea* L. leaves, and chemical analysis of the essential oil. *Ann. Bot.* **1997**, *79*, 329–336.
 100. Gul, S.; Ahmad, M.; Zafar, M.; et al. Foliar epidermal anatomy of Lamiaceae with special emphasis on their trichomes diversity using scanning electron microscopy. *Microsc. Res. Tech.* **2019**, *82*, 206–223.
 101. Karabourniotis, G.; Liakopoulos, G.; Nikolopoulos, D.; et al. Protective and defensive roles of non-glandular trichomes against multiple stresses: Structure–function coordination. *J. For. Res.* **2020**, *31*, 1–12.
 102. Mahmoud, S.S.; Maddock, S.; Adal, A.M. Isoprenoid Metabolism and Engineering in Glandular Trichomes of *Lamiaceae*. *Front. Plant Sci.* **2021**, *12*, 699157.
 103. Wang, X.; Shen, C.; Meng, P.; et al. Analysis and review of trichomes in plants. *BMC Plant Biol.* **2021**, *21*, 70.
 104. Tirillini, B.; Maggi, F. Volatile Organic Compounds of the Glandular Trichomes of *Ocimum basilicum* and Artifacts during the Distillation of the Leaves. *Appl. Sci.* **2021**, *11*, 7312.
 105. Schillmiller, A.L.; Last, R.L.; Pichersky, E. Harnessing plant trichome biochemistry for the production of useful compounds. *Plant J.* **2008**, *54*, 702–711.
 106. Weathers, P.J.; Arsenault, P.R.; Covello, P.S.; et al. Artemisinin production in *Artemisia annua*: Studies in planta and results of a novel delivery method for treating malaria and other neglected diseases. *Phytochem. Rev.* **2011**, *10*, 173–183.
 107. Moon, H.-K.; Hong, S.-P.; Smets, E.; et al. Phylogenetic Significance of Leaf Micromorphology and Anatomy in the Tribe Mentheae (Nepetoideae: Lamiaceae). *Bot. J. Linn. Soc.* **2009**, *160*, 211–231.
 108. Abu-Assab, M.S.; Cantino, P.D. Phylogenetic Implications of Leaf Anatomy in Subtribe Melittidinae (Labiatae) and Related Taxa. *J. Arnold Arbor.* **1987**, *68*, 1–34.
 109. Khosroshahi E.E.; Salmaki, Y. Evolution of trichome types and its systematic significance in the genus *Phlomis* (Lamiaceae–Lamiaceae). *Nord. J. Bot.* **2019**, *37*. <https://doi.org/10.1111/njb.02132>.
 110. Majeed, J.; Shaheen, S.; Waheed, M.; et al. Morpho-anatomical studies of family lamiaceae species of district Lahore, Punjab: A revision to flora of Pakistan. *BMC Plant Biol.* **2024**, *24*, 694.
 111. Maurya, S.; Chandra, M.; Yadav, R.K.; et al. Interspecies comparative features of trichomes in *Ocimum* reveal insights for biosynthesis of specialized essential oil metabolites. *Protoplasma* **2019**, *256*, 893–907.
 112. Gang, D.R.; Simon, J.; Lewinsohn, E.; et al. Peltate Glandular Trichomes of *Ocimum basilicum* L. (Sweet Basil) Contain High Levels of Enzymes Involved in the Biosynthesis of Phenylpropanes. *J. Herbs Spices Med. Plants* **2002**, *9*, 189–195.

113. Punja, Z.K.; Sutton, D.B.; Kim, T. Glandular trichome development, morphology, and maturation are influenced by plant age and genotype in high THC-containing cannabis (*Cannabis sativa* L.) inflorescences. *J. Cannabis Res.* **2023**, *5*, 12.
114. Di Cesare, L.F.; Forni, E.; Viscardi, D.; et al. Changes in the chemical composition of Basil caused by different drying procedures. *J. Agric. Food Chem.* **2003**, *51*, 3575–3581.
115. Das, P.C.; Vista, A.R.; Tabil, L.G.; et al. Postharvest operations of Cannabis and their effect on cannabinoid content: A Review. *Bioengineering* **2022**, *9*, 364.
116. Mokhtarikhah, G.; Ebadi, M-T., Ayyari, M. Qualitative changes of spearmint essential oil as affected by drying methods. *Ind. Crops Prod.* **2020**, *153*, 112492.
117. El-Gamal, R.; Song, C.; Rayan, A.M.; et al. Thermal Degradation of Bioactive Compounds during Drying Process of Horticultural and Agronomic Products: A Comprehensive Overview. *Agronomy* **2023**, *13*, 1580.
118. dos Santos Tozin, L.R.; Tatiane, M.R. Glandular trichomes in the tree-basil (*Ocimum gratissimum* L., Lamiaceae): Morphological features with emphasis on the cytoskeleton. *Flora* **2019**, *259*, 151459.
119. Huchelmann, A.; Boutry, M.; Hachez, C. Plant Glandular Trichomes: Natural Cell Factories of High Biotechnological Interest. *Plant Physiol.* **2017**, *175*, 6–22.
120. Han, G.; Li, Y.; Yang, Z.; et al. Molecular Mechanisms of Plant Trichome Development. *Front. Plant Sci.* **2022**, *13*, 910228.
121. Watts, S.; Kariyat, R. Morphological characterization of trichomes shows enormous variation in shape, density and dimensions across the leaves of 14 *Solanum* species. *AoB Plants*, **2021**, *13*, plab071.
122. Feng, Z.; Bartholomew, E.S.; Liu, Z.; et al. Glandular trichomes: New focus on horticultural crops. *Hortic. Res.* **2021**, *8*, 158.
123. De Masi, L.; Siviero, P.; Esposito, C.; et al. Assessment of agronomic, chemical and genetic variability in common basil (*Ocimum basilicum* L.) *Eur. Food Res. Technol.* **2006**, *223*, 273–281.
124. Ciriello, M.; Pannico, A.; El-Nakhel, C.; et al. Sweet Basil Functional Quality as Shaped by Genotype and Macronutrient Concentration Reciprocal Action. *Plants* **2020**, *9*, 1786.
125. Tammannavar, P.; Pushpalatha, C.; Jain, S.; et al. An unexpected positive hypersensitive reaction to eugenol. *BMJ Case Rep.* **2013**, bcr2013009464. <https://doi.org/10.1136/bcr-2013-009464>.
126. Iijima, Y.; Davidovich-Rikanati, R.; Fridman, E.; et al. The biochemical and molecular basis for the divergent patterns in the biosynthesis of terpenes and phenylpropenes in the peltate glands of three cultivars of basil. *Plant Physiol.* **2004**, *136*, 3724–3736.
127. Pichersky, E.; Noel, J.P.; Dudareva, N. Biosynthesis of Plant Volatiles: Nature's Diversity and Ingenuity. *Science* **2006**, *311*, 808–811.
128. Kısa, D.; Ceylan, Y.; İmamoğlu, R. Accumulation of phenolic compounds and expression of phenylpropanoid biosynthesis-related genes in leaves of basil transformed with *A. rhizogenes* strains. *Physiol. Mol. Biol. Plants* **2023**, *29*, 629–640.
129. Gang, D.R.; Lavid, N.; Zubieta, C.; et al. Characterization of phenylpropene O-methyltransferases from sweet basil: Facile change of substrate specificity and convergent evolution within a plant O-methyltransferase family. *Plant Cell* **2002**, *14*, 505–519.
130. Tremmel, R.; Herrmann, K.; Engst, W.; et al. Methyleugenol DNA adducts in human liver are associated with SULT1A1 copy number variations and expression levels. *Arch. Toxicol.* **2017**, *91*, 3329–3339.
131. European Commission Health & Consumer Protection Directorate-General. *Opinion of the Scientific Committee on Food on Estragole (1-Allyl-4-methoxybenzene)*; Scientific Committee on Food: Brussel, Belgium, 2001.
132. National Toxicology Program (NTP). *Toxicology and Carcinogenesis Studies of Methyleugenol (CAS No. 93-15-2) in F344/N Rats and B6C3F1 Mice (Gavage Studies)*; Technical Report Series No. 491; NTP: Research Triangle Park, NC, USA, 2000.
133. Vural, N. Chemometrics data analysis and controversial carcinogenic effect of *Ocimum basilicum* L. rich in methyl eugenol. *Food Meas.* **2021**, *15*, 4825–4837.
134. Kofidis, G.; Bosabalidis, A.; Kokkini, S. Seasonal Variation of Essential Oils in a Linalool-Rich Chemotype of *Mentha spicata* Grown Wild in Greece. *J. Essent. Oil Res.* **2004**, *16*, 469–472.
135. Anand, A.; Jayaramaiah, R.H.; Beedkar, S.D.; et al. Comparative functional characterization of eugenol synthase from four different *Ocimum* species: Implications on eugenol accumulation. *Biochim. Biophys. Acta* **2016**, *1864*, 1539–1547.
136. Kamatou, G.P.P.; Viljoen, A.M. Linalool—A Review of a Biologically Active Compound of Commercial Importance. *Nat. Prod. Commun.* **2008**, *3*, 1183–1192.
137. Dos Santos, É.R.Q.; Maia, J.G.S.; Fontes-Júnior, E.A.; et al. Linalool as a Therapeutic and Medicinal Tool in Depression Treatment: A Review. *Curr. Neuropharmacol.* **2022**, *20*, 1073–1092.
138. Radulović, N.S.; Blagojević, P.D.; Miltojević, A.B. α -Linalool—A marker compound of forged/synthetic sweet basil (*Ocimum basilicum* L.) essential oils. *J. Sci. Food Agric.* **2013**, *93*, 3292–3303.
139. Mączka, W.; Duda-Madej, A.; Grabarczyk, M.; et al. Natural Compounds in the Battle against Microorganisms—Linalool. *Molecules* **2022**, *27*, 6928.

140. Türkmen, M. The effect of different Phenological periods and harvest times on the essential oil ratio and components of basil genotypes. *J. Essent. Oil-Bear. Plants*. **2021**, *24*, 94–109.
141. Hazrati, S.; Mousavi, Z.; Nicola, S. Harvest time optimization for medicinal and aromatic plant secondary metabolites. *Plant Physiol. Biochem*. **2024**, *212*, 108735.
142. Bai, C.; Yang, J.; Cao, B.; et al. Growth years and post-harvest processing methods have critical roles on the contents of medicinal active ingredients of *Scutellaria baicalensis*. *Ind. Crops Prod*. **2020**, *158*, 112985.
143. Xing, Z.; Bi, G.; Li, T.; et al. Effect of Harvest Time on Growth and Bioactive Compounds in *Salvia miltiorrhiza*. *Plants* **2024**, *13*, 1788.
144. Heinrich, M.; Barnes, J.; Prieto-Garcia, J.; et al. *Fundamentals of Pharmacognosy and Phytotherapy: Fundamentals of Pharmacognosy and Phytotherapy E-Book*, 3rd ed.; Elsevier Health Sciences: London, UK, 2017.
145. De Vincenzi, M.; Silano, M.; Maialelli, F.; et al. Constituents of aromatic plants: II. Estragole. *Fitoterapia*. **2001**, *71*, 725–729.
146. Upton R.; David, B.; Gafner, S.; et al. Botanical Ingredient Identification and Quality Assessment: Strengths and Limitations of Analytical Techniques. *Phytochem. Rev*. **2020**, *19*, 1157–1177.
147. Simmler, C.; Chen, S.N.; Anderson, J.; et al. Botanical Integrity: The Importance of the Integration of Chemical, Biological, and Botanical Analyses, and the Role of DNA Barcoding. *HerbalGram* **2015**, *106*, 58–60.
148. Dawan, J.; Ahn, J. Application of DNA barcoding for ensuring food safety and quality. *Food Sci. Biotechnol*. **2022**, *31*, 1355–1364.
149. Ragupathy, S.; Thirugnanasambandam, A.; Henry, T.; et al. Flower Species Ingredient Verification Using Orthogonal Molecular Methods. *Food* **2024**, *13*, 1862.
150. Mück, F.; Scotti, F.; Mauvisseau, Q.; et al. Three-Tiered Authentication of Herbal Traditional Chinese Medicine Ingredients Used in Women's Health Provides Progressive Qualitative and Quantitative Insight. *Front. Pharmacol*. **2024**, *15*, 1353434.
151. Kress, W.J.; Wurdack, K.J.; Zimmer, E.A.; et al. Use of DNA barcodes to identify flowering plants. *Proc. Natl. Acad. Sci. USA* **2005**, *102*, 8369–8374.